Applied Mathematics and Computation 404 (2021) 126251

Contents lists available at ScienceDirect

Applied Mathematics and Computation

journal homepage: www.elsevier.com/locate/amc

Short-term predictions and prevention strategies for COVID-19: A model-based study

Sk Shahid Nadim[a], Indrajit Ghosh[b,*], Joydev Chattopadhyay[a]

[a] Agricultural and Ecological Research Unit, Indian Statistical Institute, Kolkata 700108, West Bengal, India
[b] Department of Computational and Data Sciences, Indian Institute of Science, Bengalore 560012, Karnataka, India

ARTICLE INFO

Article history:
Received 23 July 2020
Revised 18 March 2021
Accepted 28 March 2021
Available online 1 April 2021

Keywords:
Coronavirus disease
Mathematical model
Basic reproduction number
Model calibration and prediction
Control strategies
United Kingdom

ABSTRACT

An outbreak of respiratory disease caused by a novel coronavirus is ongoing from December 2019. As of December 14, 2020, it has caused an epidemic outbreak with more than 73 million confirmed infections and above 1.5 million reported deaths worldwide. During this period of an epidemic when human-to-human transmission is established and reported cases of coronavirus disease 2019 (COVID-19) are rising worldwide, investigation of control strategies and forecasting are necessary for health care planning. In this study, we propose and analyze a compartmental epidemic model of COVID-19 to predict and control the outbreak. The basic reproduction number and the control reproduction number are calculated analytically. A detailed stability analysis of the model is performed to observe the dynamics of the system. We calibrated the proposed model to fit daily data from the United Kingdom (UK) where the situation is still alarming. Our findings suggest that independent self-sustaining human-to-human spread ($R_0 > 1$, $R_c > 1$) is already present. Short-term predictions show that the decreasing trend of new COVID-19 cases is well captured by the model. Further, we found that effective management of quarantined individuals is more effective than management of isolated individuals to reduce the disease burden. Thus, if limited resources are available, then investing on the quarantined individuals will be more fruitful in terms of reduction of cases.

1. Introduction

In December 2019, an outbreak of coronavirus disease (COVID-19), was first noted in Wuhan, Central China [1]. The outbreak was declared a public health emergency of international concern on 30 January 2020 by WHO. Coronaviruses belong to the Coronaviridae family and widely distributed in humans and other mammals [31]. The virus is responsible for a range of symptoms including dry cough, fever, fatigue, breathing difficulty, and bilateral lung infiltration in severe cases, similar to those caused by Severe Acute Respiratory Syndrome Coronavirus (SARS-CoV) and Middle East Respiratory Syndrome Coronavirus (MERS-CoV) infections [27,31]. Many people may experience non-breathing symptoms including nausea, vomiting and diarrhea [3]. Some patients have reported radiographic changes in their ground-glass lungs; normal or lower than average white blood cell lymphocyte, and platelet counts; hypoxaemia; and deranged liver and renal function. Most of them were said to be geographically connected to the Huanan seafood wholesale market, which was subsequently claimed by journalists to be selling freshly slaughtered game animals [2]. The Chinese health authority said the patients initially tested negative

* Corresponding author.
E-mail addresses: indra7math@gmail.com, indrajitg_r@isical.ac.in (I. Ghosh).

https://doi.org/10.1016/j.amc.2021.126251
0096-3003/

for common respiratory viruses and bacteria but subsequently tested positive for a novel coronavirus [16]. The SARS-CoV-2 virus spreads from person to person as confirmed in [16]. It has become an epidemic outbreak with more than 73 million confirmed infections and above 1.5 million deaths worldwide as of 14 December 2020. The current epidemic outbreak result in 1,869,666 confirmed cases and 64,402 deaths in the UK [4].

Since the first discovery and identification of coronavirus in 1965, three major outbreaks occurred, caused by emerging, highly pathogenic coronaviruses, namely the 2003 outbreak of SARS-CoV in mainland China [28,39], the 2012 outbreak of MERS-CoV in Saudi Arabia [23,49], and the 2015 outbreak of MERS-CoV in South Korea [21,34]. These outbreaks resulted in SARS-CoV and MERS-CoV cases confirmed by more than 8000 and 2200, respectively [37]. The COVID-19 is caused by a new genetically similar coronavirus to the viruses that cause SARS-CoV and MERS-CoV. Despite a relatively lower death rate compared to SARS-CoV and MERS-CoV, the COVID-19 spreads rapidly and infects more people than the SARS-CoV and MERS-CoV outbreaks. In spite of strict intervention measures implemented in the region where the infection originated, the infection spread locally in Wuhan, in China and around globally.

On 31 January 2020, the UK reported the first confirmed case of acute respiratory infection due to coronavirus disease 2019 (COVID-19) and initially responded to the spread of infection by quarantining at-risk individuals. As of 14 December 2020, there were 1,869,666 confirmed cases and 64,402 confirmed deaths [4]. Within the hospitals, the infection rate is higher than in the population. On March 23, the UK government implemented a lock-down and declared that everyone should start social distancing immediately, suggesting that contact with others will be avoided as far as possible. Entire households should also quarantine themselves for 14 days if anyone has a symptom of COVID-19, and anyone at high risk of serious illness should isolate themselves for 12 weeks, including pregnant women, people over 70 and those with other health conditions. The country is literally at a standstill and the disease has seriously impacted the economy and the livelihood of the people.

As the COVID-19 is expanding rapidly in UK, real-time analyzes of epidemiological data are required to increase situational awareness and inform interventions. Earlier, in the first few weeks of an outbreak, real-time analysis shed light on the severity, transmissibility, and natural history of an emerging pathogen, such as SARS-CoV, the 2009 influenza pandemic, and Ebola [18,19,26,40]. Analysis of detailed patient line lists is especially useful for inferring key epidemiological parameters, such as infectious and incubation periods, and delays between infection and detection, isolation and case reporting [18,19]. However, official patient's health data seldom become available to the public early in an outbreak, when the information is most required. In addition to medical and biological research, theoretical studies based on either mathematical or statistical modeling may also play an important role throughout this anti-epidemic fight in understanding the epidemic character traits of the outbreak, in predicting the inflection point and end time, and in having to decide on the measures to reduce the spread. To this end, many efforts have been made at the early stage to estimate key epidemic parameters and forecast future cases in which the statistical models are mostly used [15,38,44]. An Imperial College London study group calculated that 4000 (95% CI: 1000–9700) cases had occurred in Wuhan with symptoms beginning on January 18, 2020, and an estimated basic reproduction number was 2.6 (95% CI: 1.5-3.5) using the number of cases transported from Wuhan to other countries [32]. Leung et al. reached a similar finding, calculating the number of cases transported from Wuhan to other major cities in China [6] and also suggesting the possibility for the spreading of risk [11] for travel-related diseases. Mathematical modeling based on dynamic equations [7,12,36,45,46,50,51] may provide detailed mechanism for the disease dynamics. However, several studies were based on the UK COVID-19 situation [20,22,33,35]. Davies et. al [22] studied the potential impact of different control measures for mitigating the burden of COVID-19 in the UK. They used a stochastic age-structured transmission model to explore a range of intervention scenarios. These studies have broadly suggested that control measures could reduce the burden of COVID-19. However, there is a scope of comparing popular intervention strategies namely, quarantine and isolation utilizing recent epidemic data from the UK.

In this study, we aim to study the control strategies that can significantly reduce the outbreak using a mathematical modeling framework. By mathematical analysis of the proposed model, we would like to explore transmission dynamics of the virus among humans. Another goal is the short-term prediction of new COVID-19 cases in the UK.

2. Model formulation

General mathematical models for the spread of infectious diseases have been described previously [25,30,41]. The well-known SEIR (Susceptible-Exposed-Infectious-Recovered) model has been developed by Wu et al. [55] to explain the transmission dynamics and to estimate the national and global spread of COVID-19, based on recorded data from 31 December 2019 to 28 January 2020. According to their study, the basic reproductive number for COVID-19 was found to be around 2.68. Read et al. [47] registered a value of 3.1 for the basic reproduction number based on the SEIR model, using an approximation of Poisson-distributed daily time increments. A sequence of SEIR models was designed and developed by Chen et al. [17] to explain the mechanisms of its transmission from the source of infection, reservoir, hosts to humans, since the mathematical model can draw known and definite conclusions about the outbreak of COVID-19. A generalised time-varying SEIR disease model subject to delays, which may include mixed regular and impulsive vaccination laws, was discussed in [24]. L.H.A. Monteiro investigates a SAIR epidemic model of COVID-19, which specifically takes into account four pathways of person-to-person transmission involving asymptomatic and symptomatic individuals [42]. This study shows an oscillatory convergence to the endemic steady-state, which suggests the presence of a sequence of peaks as time passes in the number of infected people. In another study, L.H.A. Monteiro et al. proposed and simulated a SAIR epidemic model based

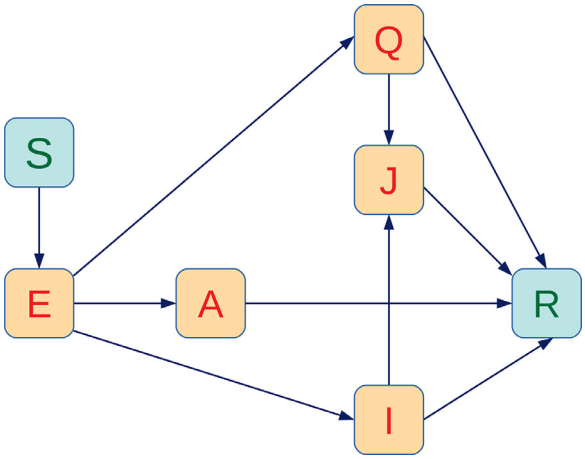

Fig. 1. Compartmental flow diagram of the proposed model.

on PCA for the spread of COVID-19 [43]. This research discussed the long-term behavior of this contagious infection and, unfortunately, its transitory phase is still going on. However, we have proposed a new SEIR model for COVID-19 in the current manuscript. Two distinct classes namely, quarantine and isolation individuals are newly incorporated in the general SEAIR (Susceptible-Exposed-Asymptomatic-Infectious-Recovered) model. Here we emphasize that after successful contact, four classes of quarantine, asymptomatic, symptomatic and isolated hospitalised populations can spread the diseases to susceptible people at different intensity. Therefore, the model monitors the dynamics of seven sub-populations, namely susceptible ($S(t)$), exposed ($E(t)$), quarantined ($Q(t)$), asymptomatic ($A(t)$), symptomatic ($I(t)$), isolated ($J(t)$) and recovered ($R(t)$) individuals. The total population size is $N(t) = S(t) + E(t) + Q(t) + A(t) + I(t) + J(t) + R(t)$. In this model, quarantine refers to the separation of COVID-19 infected individuals from the general population when the populations are infected but not infectious, whereas isolation describes the separation of COVID-19 infected individuals when the populations become symptomatic infectious. Our model incorporates some demographic effects by assuming a proportional natural death rate $\mu > 0$ in each of the seven sub-populations of the model. In addition, our model includes a net inflow of susceptible individuals into the region at a rate Π per unit time. This parameter includes new births, immigration and emigration. The flow diagram of the proposed model is displayed in Fig. 1.

Susceptible population (S(t)):

By recruiting individuals into the region, the susceptible population is increased and reduced by natural death. Also, the susceptible population decreases after infection, acquired through interaction between a susceptible individual and an infected person who may be quarantined, asymptomatic, symptomatic, or isolated. For these four groups of infected individuals, the transmission coefficients are β, $r_Q\beta$, $r_A\beta$, and $r_J\beta$ respectively. We consider the β as a transmission rate along with the modification factors for quarantined r_Q, asymptomatic r_A and isolated r_J individuals. The interaction between infected individuals (quarantined, asymptomatic, symptomatic or isolated) and susceptible is modeled in the form of total population without quarantined and isolated individuals using standard mixing incidence [25,30,41]. The rate of change of the susceptible population can be expressed by the following equation:

$$\frac{dS}{dt} = \Pi - \frac{S(\beta I + r_Q\beta Q + r_A\beta A + r_J\beta J)}{N} - \mu S, \tag{2.1}$$

Exposed population(E(t)):

Population who are exposed are infected individuals but not infectious for the community. The exposed population decreases with quarantine at a rate of γ_1, and become asymptomatic and symptomatic at a rate k_1 and natural death at a rate μ. Hence,

$$\frac{dE}{dt} = \frac{S(\beta I + r_Q\beta Q + r_A\beta A + r_J\beta J)}{N} - (\gamma_1 + k_1 + \mu)E \tag{2.2}$$

Quarantine population (Q(t)):

These are exposed individuals who are quarantined at a rate γ_1. For convenience, we consider that all quarantined individuals are exposed who will begin to develop symptoms and then transfer to the isolated class. Assuming that acertain portion ofuninfected individuals are also quarantined would be more plausible, but this would drastically complicate the model and require the introduction of many parameters and compartments. In addition, the error caused by our simplification is to leave certain people in the susceptible population who are currently in quarantine and therefore make less contacts. The population is reduced by the growth of clinical symptoms at a rate of k_2 and transferred to the isolated class.

σ_1 is the recovery rate of quarantine individuals and μ is the natural death rate of the human population. Thus,

$$\frac{dQ}{dt} = \gamma_1 E - (k_2 + \sigma_1 + \mu)Q \tag{2.3}$$

Asymptomatic population(A(t)):

Asymptomatic individuals were exposed to the virus but clinical signs of COVID have not yet developed. The exposed individuals become asymptomatic at a rate k_1 by a proportion p. The recovery rate of asymptomatic individuals is σ_2 and the natural death rate is μ. Thus,

$$\frac{dA}{dt} = pk_1 E - (\sigma_2 + \mu)A \tag{2.4}$$

Symptomatic population(I(t)):

The symptomatic individuals are produced by a proportion of $(1-p)$ of exposed class after the exposer of clinical symptoms of COVID by exposed individuals. γ_2 is the isolation rate of the symptomatic individuals, σ_3 is the recovery rate and natural death at a rate μ. Thus,

$$\frac{dI}{dt} = (1-p)k_1 E - (\gamma_2 + \sigma_3 + \mu)I \tag{2.5}$$

Isolated population(J(t)):

The isolated individuals are those who have been developed by clinical symptoms and been isolated at the hospital. The isolated individuals have come from quarantined communities at a rate k_2 and symptomatic group at a rate γ_2. The recovery rate of isolated individuals is σ_4, disease induced death rate is δ and natural death rate is μ. Thus,

$$\frac{dJ}{dt} = k_2 Q + \gamma_2 I - (\delta + \sigma_4 + \mu)J \tag{2.6}$$

Recovered population(R(t)):

Quarantined, asymptomatic, symptomatic and isolated individuals recover from the disease at rates σ_1, σ_2, σ_3 and σ_4; respectively, and this population is reduced by a natural death rate μ. It is still unclear whether the immunity due to COVID-19 is life-long or not, and hence we do not consider immunity loss in the present study. Therefore, recovered persons will not get infected even if they contact with infectious people. Thus,

$$\frac{dR}{dt} = \sigma_1 Q + \sigma_2 A + \sigma_3 I + \sigma_4 J - \mu R \tag{2.7}$$

From the above considerations, the following system of ordinary differential equations governs the dynamics of the system:

$$\begin{aligned}
\frac{dS}{dt} &= \Pi - \frac{S(\beta I + r_Q \beta Q + r_A \beta A + r_J \beta J)}{N} - \mu S,\\
\frac{dE}{dt} &= \frac{S(\beta I + r_Q \beta Q + r_A \beta A + r_J \beta J)}{N} - (\gamma_1 + k_1 + \mu)E,\\
\frac{dQ}{dt} &= \gamma_1 E - (k_2 + \sigma_1 + \mu)Q,\\
\frac{dA}{dt} &= pk_1 E - (\sigma_2 + \mu)A,\\
\frac{dI}{dt} &= (1-p)k_1 E - (\gamma_2 + \sigma_3 + \mu)I,\\
\frac{dJ}{dt} &= k_2 Q + \gamma_2 I - (\delta + \sigma_4 + \mu)J,\\
\frac{dR}{dt} &= \sigma_1 Q + \sigma_2 A + \sigma_3 I + \sigma_4 J - \mu R,
\end{aligned} \tag{2.8}$$

All the parameters and their biological interpretation are given in Table 1 respectively.

3. Mathematical analysis

3.1. Positivity and boundedness of the solution

This subsection is provided to prove the positivity and boundedness of solutions of the system (2.8) with initial conditions $(S(0), E(0), Q(0), A(0), I(0), J(0), R(0))^T \in \mathbb{R}^7_+$. We first state the following lemma.

Lemma 3.1. *Suppose* $\Omega \subset \mathbb{R} \times \mathbb{C}^n$ *is open,* $f_i \in C(\Omega, \mathbb{R}), i = 1, 2, 3, \ldots, n$. *If* $f_i|_{x_i(t)=0, X_t \in \mathbb{C}^n_{+0}} \geq 0$, $X_t = (x_{1t}, x_{2t}, \ldots., x_{1n})^T, i = 1, 2, 3, \ldots., n$, *then* $\mathbb{C}^n_{+0}\{\phi = (\phi_1, \ldots., \phi_n) : \phi \in \mathbb{C}([-\tau, 0], \mathbb{R}^n_{+0})\}$ *is the invariant domain of the following equations*

$$\frac{dx_i(t)}{dt} = f_i(t, X_t), t \geq \sigma, i = 1, 2, 3, \ldots, n.$$

where $\mathbb{R}^n_{+0} = \{(x_1, \ldots .x_n) : x_i \geq 0, i = 1, \ldots ., n\}$ *[56].*

Proposition 1. *The system (2.8) is invariant in* $\mathbb{R}^7_+$.

Proof. By re-writing the system (2.8) we have

$$\frac{dX}{dt} = M(X(t)), X(0) = X_0 \geq 0 \tag{3.1}$$

$M(X(t)) = (M_1(X), M_2(X), \ldots, M_7(X))^T$

We note that

$$\frac{dS}{dt}|_{S=0} = \Pi \geq 0, \frac{dE}{dt}|_{E=0} = \frac{S(\beta I + r_Q\beta Q + r_A\beta A + r_J\beta J)}{S+Q+A+I+J+R} \geq 0,$$
$$\frac{dQ}{dt}|_{Q=0} = \gamma_1 E \geq 0, \frac{dA}{dt}|_{A=0} = pk_1E \geq 0, \frac{dI}{dt}|_{I=0} = (1-p)k_1E \geq 0,$$
$$\frac{dJ}{dt}|_{J=0} = k_2Q + \gamma_2 I \geq 0, \frac{dR}{dt}|_{R=0} = \sigma_1 Q + \sigma_2 A + \sigma_3 I + \sigma_4 J \geq 0.$$

Then it follows from the Lemma 3.1 that $\mathbb{R}^7_+$ is an invariant set. □

Proposition 2. *The system (2.8) is bounded in the region*
$\Omega = \{(S, E, Q, A, I, J, R) \in \mathbb{R}^7_+ | S + E + Q + A + I + J + R \leq \frac{\Pi}{\mu}\}$

Proof. We observed from the system that

$$\frac{dN}{dt} = \Pi - \mu N - \delta J \leq \Pi - \mu N$$
$$\Longrightarrow \lim_{t\to\infty} supN(t) \leq \frac{\Pi}{\mu}$$

Hence the system (2.8) is bounded. □

3.2. Diseases-free equilibrium and control reproduction number

The diseases-free equilibrium can be obtained for the system (2.8) by putting $E = 0, Q = 0, A = 0, I = 0, J = 0$, which is denoted by $P^0_1 = (S^0, 0, 0, 0, 0, 0, R^0)$, where

$$S^0 = \frac{\Pi}{\mu}, R^0 = 0.$$

The control reproduction number, a central concept in the study of the spread of communicable diseases, is e the number of secondary infections caused by a single infective in a population consisting essentially only of susceptibles with the control measures in place (quarantined and isolated class) [53]. This dimensionless number is calculated at the DFE by next generation operator method [25,54] and it is denoted by R_c.

For this, we assemble the compartments which are infected from the system (2.8) and decomposing the right hand side as $\mathcal{F} - \mathcal{V}$, where $\mathcal{F}$ is the transmission part, expressing the production of new infection, and the transition part is $\mathcal{V}$, which describe the change in state.

$$\mathcal{F} = \begin{pmatrix} \frac{S(\beta I + r_Q\beta Q + r_A\beta A + r_J\beta J)}{N} \\ 0 \\ 0 \\ 0 \\ 0 \end{pmatrix}, \mathcal{V} = \begin{pmatrix} (\gamma_1 + k_1 + \mu)E \\ -\gamma_1 E + (k_2 + \sigma_1 + \mu)Q \\ -pk_1E + (\sigma_2 + \mu)A \\ -(1-p)k_1E + (\gamma_2 + \sigma_3 + \mu)I \\ -k_2Q - \gamma_2 I + (\delta + \sigma_4 + \mu)J \end{pmatrix}$$

Now we calculate the jacobian of $\mathcal{F}$ and $\mathcal{V}$ at DFE P^0_1

$$F = \frac{\partial \mathcal{F}}{\partial X} = \begin{pmatrix} 0 & r_Q\beta & r_A\beta & \beta & r_J\beta \\ 0 & 0 & 0 & 0 & 0 \\ 0 & 0 & 0 & 0 & 0 \\ 0 & 0 & 0 & 0 & 0 \\ 0 & 0 & 0 & 0 & 0 \end{pmatrix},$$

$$V = \frac{\partial \mathcal{V}}{\partial X} = \begin{pmatrix} \gamma_1 + k_1 + \mu & 0 & 0 & 0 & 0 \\ -\gamma_1 & k_2 + \sigma_1 + \mu & 0 & 0 & 0 \\ -pk_1 & 0 & \sigma_2 + \mu & 0 & 0 \\ -(1-p)k_1 & 0 & 0 & \gamma_2 + \sigma_3 + \mu & 0 \\ 0 & -k_2 & 0 & -\gamma_2 & \delta + \sigma_4 + \mu \end{pmatrix}.$$

Following [29], $R_c = \rho(FV^{-1})$, where ρ is the spectral radius of the next-generation matrix (FV^{-1}). Thus, from the model (2.8), we have the following expression for R_c:

$$\begin{aligned} R_c = & \frac{r_Q\beta\gamma_1}{(\gamma_1+k_1+\mu)(k_2+\sigma_1+\mu)} + \frac{r_A\beta pk_1}{(\gamma_1+k_1+\mu)(\sigma_2+\mu)} \\ & + \frac{\beta k_1(1-p)}{(\gamma_1+k_1+\mu)(\gamma_2+\sigma_3+\mu)} + \frac{r_J\beta\gamma_1k_2}{(\gamma_1+k_1+\mu)(k_2+\sigma_1+\mu)(\delta+\sigma_4+\mu)} \\ & + \frac{r_J\beta(1-p)k_1\gamma_2}{(\gamma_1+k_1+\mu)(\gamma_2+\sigma_3+\mu)(\delta+\sigma_4+\mu)} \end{aligned} \tag{3.2}$$

3.3. Stability of DFE

Theorem 3.1. *The diseases free equilibrium(DFE) $P_1^0 = (S^0, 0, 0, 0, 0, 0, R^0)$ of the system (2.8) is locally asymptotically stable if $R_c < 1$ and unstable if $R_c > 1$.*

Proof. We calculate the Jacobian of the system (2.8) at DFE, and is given by

$$J_{P_1^0} = \begin{pmatrix} -\mu & 0 & -r_Q\beta & -r_A\beta & -\beta & -r_J\beta & 0 \\ 0 & -(\gamma_1+k_1+\mu) & r_Q\beta & r_A\beta & \beta & r_J\beta & 0 \\ 0 & \gamma_1 & -(k_2+\sigma_1+\mu) & 0 & 0 & 0 & 0 \\ 0 & pk_1 & 0 & -(\sigma_2+\mu) & 0 & 0 & 0 \\ 0 & (1-p)k_1 & 0 & 0 & -(\gamma_2+\sigma_3+\mu) & 0 & 0 \\ 0 & 0 & k_2 & 0 & \gamma_2 & -(\delta+\sigma_4+\mu) & 0 \\ 0 & 0 & \sigma_1 & \sigma_2 & \sigma_3 & \sigma_4 & -\mu \end{pmatrix},$$

Let λ be the eigenvalue of the matrix $J_{P_1^0}$. Then the characteristic equation is given by $det(J_{P_1^0} - \lambda I) = 0$.

$\Rightarrow$ $r_J\beta\gamma_1k_2(\lambda+\sigma_2+\mu)(\lambda+\gamma_2+\sigma_3+\mu) + r_J\beta\gamma_2k_1(\lambda+k_2+\sigma_1+\mu)[(1-p)(\lambda+\sigma_2+\mu)] + r_A\beta pk_1(\lambda+\gamma_2+\sigma_3+\mu)(\lambda+\delta+\sigma_4+\mu)(\lambda+k_2+\sigma_1+\mu) + \beta k_1[(1-p)(\lambda+\sigma_2+\mu)](\lambda+\delta+\sigma_4+\mu)(\lambda+k_2+\sigma_1+\mu) - (\lambda+\gamma_1+k_1+\mu)(\lambda+\sigma_2+\mu)(\lambda+\gamma_2+\sigma_3+\mu)(\lambda+\delta+\sigma_4+\mu)(\lambda+k_2+\sigma_1+\mu) = 0.$

Which can be written as

$$\begin{aligned} & \frac{r_Q\beta\gamma_1}{(\lambda+\gamma_1+k_1+\mu)(\lambda+k_2+\sigma_1+\mu)} + \frac{r_A\beta pk_1}{(\lambda+\gamma_1+k_1+\mu)(\lambda+\sigma_2+\mu)} \\ & + \frac{\beta k_1(1-p)}{(\lambda+\gamma_1+k_1+\mu)(\lambda+\gamma_2+\sigma_3+\mu)} \\ & + \frac{r_J\beta\gamma_1k_2}{(\lambda+\gamma_1+k_1+\mu)(\lambda+k_2+\sigma_1+\mu)(\lambda+\delta+\sigma_4+\mu)} \\ & + \frac{r_J\beta(1-p)k_1\gamma_2}{(\lambda+\gamma_1+k_1+\mu)(\lambda+\gamma_2+\sigma_3+\mu)(\lambda+\delta+\sigma_4+\mu)} = 1 = G_1(\lambda)(say). \end{aligned}$$

We rewrite $G_1(\lambda)$ as $G_1(\lambda) = G_{11}(\lambda) + G_{12}(\lambda) + G_{13}(\lambda) + G_{14}(\lambda) + G_{15}(\lambda)$

Now if $Re(\lambda) \geq 0$, $\lambda = x + iy$, then

$$|G_{11}(\lambda)| \leq \frac{r_Q\beta\gamma_1}{|\lambda+\gamma_1+k_1+\mu||\lambda+k_2+\sigma_1+\mu|} \leq G_{11}(x) \leq G_{11}(0)$$

$$|G_{12}(\lambda)| \leq \frac{r_A\beta pk_1}{|\lambda+\gamma_1+k_1+\mu||\lambda+\sigma_2+\mu|} \leq G_{12}(x) \leq G_{12}(0)$$

$$|G_{13}(\lambda)| \leq \frac{\beta k_1(1-p)}{|\lambda+\gamma_1+k_1+\mu||\lambda+\gamma_2+\sigma_3+\mu|} \leq G_{13}(x) \leq G_{13}(0)$$

$$|G_{14}(\lambda)| \leq \frac{r_J\beta\gamma_1k_2}{|\lambda+\gamma_1+k_1+\mu||\lambda+k_2+\sigma_1+\mu||\lambda+\delta+\sigma_4+\mu|} \leq G_{14}(x) \leq G_{14}(0)$$

$$|G_{15}(\lambda)| \leq \frac{r_J\beta(1-p)k_1\gamma_2}{|\lambda+\gamma_1+k_1+\mu||\lambda+\gamma_2+\sigma_3+\mu||\lambda+\delta+\sigma_4+\mu|} \leq G_{15}(x) \leq G_{15}(0)$$

Then $G_{11}(0) + G_{12}(0) + G_{13}(0) + G_{14}(0) + G_{15}(0) = G_1(0) = R_c < 1$, which implies $|G_1(\lambda)| \leq 1$.

Thus for $R_c < 1$, all the eigenvalues of the characteristics equation $G_1(\lambda) = 1$ has negative real parts.

Therefore if $R_c < 1$, all eigenvalues are negative and hence DFE P_1^0 is locally asymptotically stable.

Now if we consider $R_c > 1$ i.e $G_1(0) > 1$, then

$$\lim_{\lambda\to\infty} G_1(\lambda) = 0.$$

Then there exist $\lambda_1^* > 0$ such that $G_1(\lambda_1^*) = 1$.

That means there exist positive eigenvalue $\lambda_1^* > 0$ of the Jacobian matrix.

Hence DFE P_1^0 is unstable whenever $R_c > 1$. □

Theorem 3.2. *The diseases free equilibrium (DFE) $P_1^0 = (S^0, 0, 0, 0, 0, 0, R^0)$ is globally asymptotically stable (GAS) for the system (2.8) if $R_c < 1$ and unstable if $R_c > 1$.*

Proof. We rewrite the system (2.8) as

$$\frac{dX}{dt} = F(X, V)$$
$$\frac{dV}{dt} = G(X, V), G(X, 0) = 0$$

where $X = (S, R) \in R_2$ (the number of uninfected individuals compartments), $V = (E, Q, A, I, J) \in R_5$ (the number of infected individuals compartments), and $P_1^0 = (\frac{\Pi}{\mu}, 0, 0, 0, 0, 0, 0)$ is the DFE of the system (2.8). The global stability of the DFE is guaranteed if the following two conditions are satisfied:

1. For $\frac{dX}{dt} = F(X, 0)$, X^* is globally asymptotically stable,
2. $G(X, V) = BV - \widehat{G}(X, V)$, $\widehat{G}(X, V) \geq 0$ for $(X, V) \in \Omega$,

where $B = D_V G(X^*, 0)$ is a Metzler matrix and Ω is the positively invariant set with respect to the model (2.8). Following Castillo-Chavez et al [13], we check for aforementioned conditions. For system (2.8),

$$F(X, 0) = \begin{pmatrix} \Pi - \mu S \\ 0 \end{pmatrix},$$

$$B = \begin{pmatrix} -(\gamma_1 + k_1 + \mu) & r_Q\beta & r_A\beta & \beta & r_J\beta \\ \gamma_1 & -(k_2 + \sigma_1 + \mu) & 0 & 0 & 0 \\ pk_1 & 0 & -(\sigma_2 + \mu) & 0 & 0 \\ (1-p)k_1 & 0 & 0 & -(\gamma_2 + \sigma_3 + \mu) & 0 \\ 0 & k_2 & 0 & \gamma_2 & -(\delta + \sigma_4 + \mu) \end{pmatrix}$$

and

$$\widehat{G}(X, V) = \begin{pmatrix} r_Q\beta Q(1 - \frac{S}{N}) + r_A\beta A(1 - \frac{S}{N}) + \beta I(1 - \frac{S}{N}) + r_J\beta J(1 - \frac{S}{N}) \\ 0 \\ 0 \\ 0 \\ 0 \end{pmatrix}.$$

Clearly, $\widehat{G}(X, V) \geq 0$ whenever the state variables are inside Ω. Also it is clear that $X^* = (\frac{\Pi}{\mu}, 0)$ is a globally asymptotically stable equilibrium of the system $\frac{dX}{dt} = F(X, 0)$. Hence, the theorem follows. □

3.4. Existence and local stability of endemic equilibrium

In this section, the existence of the endemic equilibrium of the model (2.8) is established. Let us denote

$$m_1 = \gamma_1 + k_1 + \mu, m_2 = k_2 + \sigma_1 + \mu, m_3 = \sigma_2 + \mu,$$
$$m_4 = \gamma_2 + \sigma_3 + \mu, m_5 = \delta + \sigma_4 + \mu.$$

Let $P_1^* = (S^*, E^*, Q^*, A^*, I^*, J^*, R^*)$ represents any arbitrary endemic equilibrium point (EEP) of the model (2.8). Further, define

$$\eta^* = \frac{\beta(I^* + r_Q Q^* + r_A A^* + r_J J^*)}{N^*} \tag{3.3}$$

It follows, by solving the equations in (2.8) at steady-state, that

$$S^* = \frac{\Pi}{\eta^* + \mu}, E^* = \frac{\eta^* S^*}{m_1}, Q^* = \frac{\gamma_1 \eta^* S^*}{m_1 m_2}, A^* = \frac{pk_1 \eta^* S^*}{m_1 m_3}, \tag{3.4}$$
$$I^* = \frac{(1-p)k_1 \eta^* S^*}{m_1 m_4}, J^* = \frac{\eta^* S^*(k_2\gamma_1 m_4 + (1-p)k_1\gamma_2 m_2)}{m_1 m_2 m_4 m_5}$$
$$R^* = \frac{\eta^* S^*[\sigma_1\gamma_1 m_3 m_4 m_5 + pk_1\sigma_2 m_2 m_4 m_5 + (1-p)k_1\sigma_3 m_2 m_3 m_5 + m_3\sigma_4(k_2\gamma_1 m_4 + (1-p)k_1\gamma_2 m_2)]}{\mu m_1 m_2 m_3 m_4 m_5}$$

Substituting the expression in (3.4) into (3.3) shows that the non-zero equilibrium of the model (2.8) satisfy the following linear equation, in terms of η^*:

$$A\eta^* + B = 0 \tag{3.5}$$

where

$$A = \mu[m_2m_3m_4m_5 + \gamma_1m_3m_4m_5 + pk_1m_2m_4m_5 + (1-p)k_1m_2m_3m_5 + k_2\gamma_1m_3m_4 + (1-p)k_1\gamma_2m_2m_3] + \sigma_1\gamma_1m_3m_4m_5 + \sigma_2pk_1m_2m_4m_5 + (1-p)k_1\sigma_3m_2m_3m_5 + \sigma_4k_2\gamma_1m_3m_4 + (1-p)\sigma_4\gamma_2k_1m_2m_3$$

$$B = \mu m_1m_2m_3m_4m_5(1-R_c)$$

Since $A > 0,\ \mu > 0,\ m_1 > 0,\ m_2 > 0,\ m_3 > 0,\ m_4 > 0$ and $m_5 > 0$, it is clear that the model (2.8) has a unique endemic equilibrium point (EEP) whenever $R_c > 1$ and no positive endemic equilibrium point whenever $R_c < 1$. This rules out the possibility of the existence of equilibrium other than DFE whenever $R_c < 1$. Furthermore, it can be shown that, the DFE P_1^0 of the model (2.8) is globally asymptotically stable (GAS) whenever $R_c < 1$.

From the above discussion we have concluded that

Theorem 3.3. *The model (2.8) has a unique endemic (positive) equilibrium, given by P_1^*, whenever $R_c > 1$ and has no endemic equilibrium for $R_c \leq 1$.*

Now we will prove the local stability of endemic equilibrium.

Theorem 3.4. *The endemic equilibrium P_1^* is locally asymptotically stable if $R_C > 1$.*

Proof. Let $x = (x_1, x_2, x_3, x_4, x_5, x_6, x_7)^T = (S, E, Q, A, I, J, R)^T$. Thus, the model (2.8) can be re-written in the form $\frac{dx}{dt} = f(x)$, with $f(x) = (f_1(x), \ldots., f_7(x))$, as follows:

$$\begin{aligned}
\frac{dx_1}{dt} &= \Pi - \frac{x_1(\beta x_5 + r_Q\beta x_3 + r_A\beta x_4 + r_J\beta x_6)}{x_1+x_2+x_3+x_4+x_5+x_6+x_7} - \mu x_1,\\
\frac{dx_2}{dt} &= \frac{x_1(\beta x_5 + r_Q\beta x_3 + r_A\beta x_4 + r_J\beta x_6)}{x_1+x_2+x_3+x_4+x_5+x_6+x_7} - (\gamma_1+k_1+\mu)x_2,\\
\frac{dx_3}{dt} &= \gamma_1x_2 - (k_2+\sigma_1+\mu)x_3,\\
\frac{dx_4}{dt} &= pk_1x_2 - (\sigma_2+\mu)x_4,\\
\frac{dx_5}{dt} &= (1-p)k_1x_2 - (\gamma_2+\sigma_3+\mu)x_5,\\
\frac{dx_6}{dt} &= k_2x_3 + \gamma_2x_5 - (\delta+\sigma_4+\mu)x_6,\\
\frac{dx_7}{dt} &= \sigma_1x_3 + \sigma_2x_4 + \sigma_3x_5 + \sigma_4x_6 - \mu x_7,
\end{aligned} \tag{3.6}$$

The Jacobian matrix of the system (3.6) $J_{P_1^0}$ at DFE is given by

$$J_{P_1^0} = \begin{pmatrix}
-\mu & 0 & -r_Q\beta & -r_A\beta & -\beta & -r_J\beta & 0\\
0 & -(\gamma_1+k_1+\mu) & r_Q\beta & r_A\beta & \beta & r_J\beta & 0\\
0 & \gamma_1 & -(k_2+\sigma_1+\mu) & 0 & 0 & 0 & 0\\
0 & pk_1 & 0 & -(\sigma_2+\mu) & 0 & 0 & 0\\
0 & (1-p)k_1 & 0 & 0 & -(\gamma_2+\sigma_3+\mu) & 0 & 0\\
0 & 0 & k_2 & 0 & \gamma_2 & -(\delta+\sigma_4+\mu) & 0\\
0 & 0 & \sigma_1 & \sigma_2 & \sigma_3 & \sigma_4 & -\mu
\end{pmatrix},$$

Here, we use the central manifold theory method to determine the local stability of the endemic equilibrium by taking β as bifurcation parameter [14]. Select β as the bifurcation parameter and gives critical value of β at $R_C = 1$ is given as

$$\beta^* = \frac{(\gamma_1+k_1+\mu)(k_2+\sigma_1+\mu)(\sigma_2+\mu)(\gamma_2+\sigma_3+\mu)(\delta+\sigma_4+\mu)}{[r_Q\gamma_1(\sigma_2+\mu)(\gamma_2+\sigma_3+\mu)(\delta+\sigma_4+\mu) + r_Apk_1(k_2+\sigma_1+\mu)(\gamma_2+\sigma_3+\mu)(\delta+\sigma_4+\mu) + Z]}$$

where, $Z = k_1(1-p)(k_2+\sigma_1+\mu)(\sigma_2+\mu)(\delta+\sigma_4+\mu) + r_J\gamma_1k_2(\sigma_2+\mu)(\gamma_2+\sigma_3+\mu) + r_J(1-p)k_1\gamma_2(k_2+\sigma_1+\mu)(\sigma_2+\mu)$

The Jacobian of (2.8) at $\beta = \beta^*$, denoted by $J_{P_1^0}|_{\beta=\beta^*}$ has a right eigenvector (corresponding to the zero eigenvalue) given by $w = (w_1, w_2, w_3, w_4, w_5, w_6, w_7)^T$, where

$$\begin{aligned}
w_1 &= -\frac{\gamma_1+k_1+\mu}{\mu}w_2,\ w_2 = w_2 > 0,\ w_3 = \frac{\gamma_1}{k_2+\sigma_1+\mu}w_2,\ w_4 = \frac{pk_1}{\sigma_2+\mu}w_2,\\
w_5 &= \frac{(1-p)k_1}{\gamma_2+\sigma_3+\mu}w_2,\ w_6 = \frac{k_2\gamma_1}{(\delta+\sigma_4+\mu)(k_2+\sigma_1+\mu)}w_2 + \frac{\gamma_2(1-p)k_1}{(\delta+\sigma_4+\mu)(\gamma_2+\sigma_3+\mu)}w_2\\
w_7 &= \frac{1}{\mu}\Big[\frac{\sigma_1\gamma_1}{k_2+\sigma_1+\mu}w_2 + \frac{\sigma_2pk_1}{\sigma_2+\mu}w_2 + \frac{\sigma_3(1-p)k_1}{\gamma_2+\sigma_3+\mu]w_2} + \frac{\sigma_4k_2\gamma_1}{(\delta+\sigma+\mu)(k_2+\sigma_1+\mu)}w_2
\end{aligned}$$

$$+\frac{\sigma_4\gamma_2(1-p)k_1}{(\delta+\sigma+\mu)(\gamma_2+\sigma_3+\mu)}w_2\Big].$$

Similarly, from $J_{P_1^0}|_{\beta=\beta^*}$, we obtain a left eigenvector $v=(v_1,v_2,v_3,v_4,v_5,v_6,v_7)$ (corresponding to the zero eigenvalue), where

$$v_1=0, v_2=v_2>0, v_3=\frac{r_Q\beta^*}{k_2+\sigma_1+\mu}v_2+\frac{k_2r_J\beta^*}{(k_2+\sigma_1+\mu)(\delta+\sigma_4+\mu)}v_2, v_4=\frac{r_A\beta^*}{\sigma_2+\mu}v_2,$$
$$v_5=\frac{\beta^*}{\gamma_2+\sigma_3+\mu}v_2+\frac{\gamma_2r_J\beta^*}{(\gamma_2+\sigma_3+\mu)(\delta+\sigma_4+\mu)}v_2, v_6=\frac{r_J\beta^*}{\delta+\sigma_4+\mu}v_2, v_7=0.$$

We calculate the following second order partial derivatives of f_i at the disease-free equilibrium P_1^0 to show the stability of the endemic equilibrium and obtain

$$\frac{\partial^2 f_2}{\partial x_3\partial x_2}=-\frac{\beta r_Q\mu}{\Pi}, \frac{\partial^2 f_2}{\partial x_4\partial x_2}=-\frac{\beta r_A\mu}{\Pi}, \frac{\partial^2 f_2}{\partial x_5\partial x_2}=-\frac{\beta\mu}{\Pi}, \frac{\partial^2 f_2}{\partial x_6\partial x_2}=-\frac{\beta r_J\mu}{\Pi},$$
$$\frac{\partial^2 f_2}{\partial x_2\partial x_3}=-\frac{\beta r_Q\mu}{\Pi}, \frac{\partial^2 f_2}{\partial x_3\partial x_3}=-\frac{2\beta r_Q\mu}{\pi}, \frac{\partial^2 f_2}{\partial x_4\partial x_3}=-\frac{\beta r_Q\mu}{\Pi}-\frac{\beta r_A\mu}{\Pi},$$
$$\frac{\partial^2 f_2}{\partial x_5\partial x_3}=-\frac{\beta r_Q\mu}{\Pi}-\frac{\beta\mu}{\pi}, \frac{\partial^2 f_2}{\partial x_6\partial x_3}=-\frac{\beta r_Q\mu}{\pi}-\frac{\beta r_J\mu}{\Pi}, \frac{\partial^2 f_2}{\partial x_7\partial x_3}=-\frac{\beta r_Q\mu}{\Pi}, \frac{\partial^2 f_2}{\partial x_2\partial x_4}=-\frac{\beta r_A\mu}{\Pi},$$
$$\frac{\partial^2 f_2}{\partial x_3\partial x_4}=-\frac{\beta r_A\mu}{\Pi}-\frac{\beta r_Q\mu}{\Pi}, \frac{\partial^2 f_2}{\partial x_4\partial x_4}=-\frac{2\beta r_A\mu}{\Pi}, \frac{\partial^2 f_2}{\partial x_5\partial x_4}=-\frac{\beta r_A\mu}{\Pi}-\frac{\beta\mu}{\Pi},$$
$$\frac{\partial^2 f_2}{\partial x_6\partial x_4}=-\frac{\beta r_A\mu}{\Pi}-\frac{\beta r_J\mu}{\Pi}, \frac{\partial^2 f_2}{\partial x_7\partial x_4}=-\frac{\beta r_A\mu}{\Pi}, \frac{\partial^2 f_2}{\partial x_2\partial x_5}=-\frac{\beta\mu}{\Pi},$$
$$\frac{\partial^2 f_2}{\partial x_3\partial x_5}=-\frac{\beta\mu}{\Pi}-\frac{\beta r_Q\mu}{\Pi}, \frac{\partial^2 f_2}{\partial x_4\partial x_5}=-\frac{\beta\mu}{\Pi}-\frac{\beta r_A\mu}{\Pi}, \frac{\partial^2 f_2}{\partial x_5\partial x_5}=-\frac{2\beta\mu}{\Pi},$$
$$\frac{\partial^2 f_2}{\partial x_6\partial x_5}=-\frac{\beta\mu}{\pi}-\frac{\beta r_J\mu}{\Pi}, \frac{\partial^2 f_2}{\partial x_7\partial x_5}=-\frac{\beta\mu}{\Pi}, \frac{\partial^2 f_2}{\partial x_2\partial x_6}=-\frac{\beta r_J\mu}{\Pi}, \frac{\partial^2 f_2}{\partial x_3\partial x_6}=-\frac{\beta r_J\mu}{\Pi}-\frac{\beta r_Q\mu}{\Pi},$$
$$\frac{\partial^2 f_2}{\partial x_4\partial x_6}=-\frac{\beta r_J\mu}{\Pi}-\frac{\beta r_A\mu}{\Pi}, \frac{\partial^2 f_2}{\partial x_5\partial x_6}=-\frac{\beta r_J\mu}{\Pi}-\frac{\beta\mu}{\Pi}, \frac{\partial^2 f_2}{\partial x_6\partial x_6}=-\frac{2\beta r_J\mu}{\Pi}, \frac{\partial^2 f_2}{\partial x_7\partial x_6}=-\frac{\beta r_J\mu}{\Pi},$$
$$\frac{\partial^2 f_2}{\partial x_3\partial x_7}=-\frac{\beta r_Q\mu}{\Pi}, \frac{\partial^2 f_2}{\partial x_4\partial x_7}=\frac{\beta r_A\mu}{\Pi}, \frac{\partial^2 f_2}{\partial x_5\partial x_7}=-\frac{\beta\mu}{\Pi}, \frac{\partial^2 f_2}{\partial x_6\partial x_7}=-\frac{\beta r_J\mu}{\Pi}$$

Now we calculate the coefficients a and b defined in Theorem 4.1 [14] of CastilloChavez and Song as follow

$$a=\sum_{k,i,j=1}^{7}v_kw_iw_j\frac{\partial^2 f_k(0,0)}{\partial x_i\partial x_j}$$

and

$$b=\sum_{k,i=1}^{7}v_kw_i\frac{\partial^2 f_k(0,0)}{\partial x_i\partial\beta}$$

Replacing the values of all the second-order derivatives measured at DFE and $\beta=\beta^*$, we get

$$a=-\frac{2\beta^*\mu v_2}{\Pi}(r_Qw_3+r_Aw_4+w_5+r_Jw_6)(w_2+w_3+w_4+w_5+w_6+w_7)<0$$

and

$$b=v_2(r_Qw_3+r_Aw_4+w_5+r_Jw_6)>0$$

Since $a<0$ and $b>0$ at $\beta=\beta^*$, therefore using the Remark 1 of the Theorem 4.1 stated in [14], a transcritical bifurcation occurs at $R_C=1$ and the unique endemic equilibrium is locally asymptotically stable for $R_C>1$. □

The transcritical bifurcation diagram is depicted in Fig. 2.

3.5. Threshold analysis

In this section, the impact of quarantine and isolation is measured qualitatively on the disease transmission dynamics. A threshold study of the parameters correlated with the quarantine of exposed individuals $\gamma_1$and the isolation of the infected symptomatic individuals γ_2 is performed by measuring the partial derivatives of the control reproduction number R_c with respect to these parameters. We observe that

$$\frac{\partial R_c}{\partial\gamma_1}=\frac{r_Q\beta(k_1+\mu)}{(\gamma_1+k_1+\mu)^2(k_2+\sigma_1+\mu)}-\frac{r_A\beta pk_1}{(\gamma_1+k_1+\mu)^2(\sigma_2+\mu)}-\frac{\beta k_1(1-p)}{(\gamma_1+k_1+\mu)^2(\gamma_2+\sigma_3+\mu)}$$

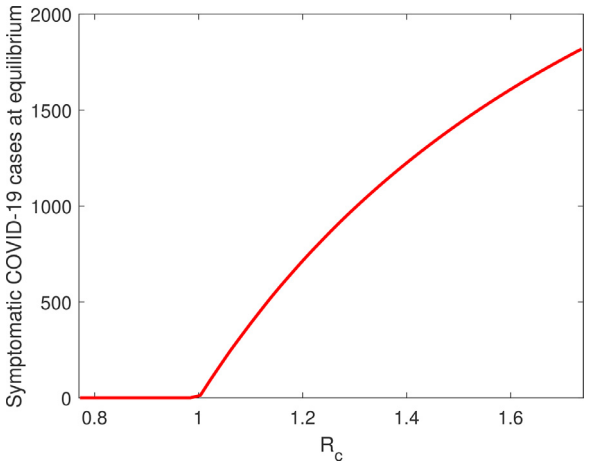

Fig. 2. Forward bifurcation diagram with respect to R_c. All the fixed parameters are taken from Table 1 with $\gamma_1 = 0.0001$, $\gamma_2 = 0.0001$, $k_2 = 0.0632$, $\sigma_1 = 0.2158$, $\sigma_2 = 0.03$ $\sigma_4 = 0.4521$ and $0.2 < \beta < 0.35$.

Table 1
Description of parameters used in the model.

Parameters	Interpretation	Value	Reference
Π	Recruitment rate	2274	[4]
β	Transmission rate	0.8883	Estimated
r_Q	Modification factor for quarantined	0.3	Assumed
r_A	Modification factor for asymptomatic	0.45	Assumed
r_J	Modification factor for isolated	0.6	Assumed
γ_1	Rate at which the exposed individuals are diminished by quarantine	0.0486	Estimated
γ_2	Rate at which the symptomatic individuals are diminished by isolation	0.1001	Estimated
k_1	Rate at which exposed become infected	1/7	[1]
k_2	Rate at which quarantined individuals are isolated	0.4129	Estimated
p	Proportion of asymptomatic individuals	0.13166	[52]
σ_1	Recovery rate from quarantined individuals	0.2553	Estimated
σ_2	Recovery rate from asymptomatic individuals	0.9982	Estimated
σ_3	Recovery rate from symptomatic individuals	0.46	[1]
σ_4	Recovery rate from isolated individuals	0.4449	Estimated
δ	Diseases induced mortality rate	0.0015	[4]
μ	Natural death rate	0.3349×10^{-4}	[5]

$$+\frac{r_J\beta}{(\gamma_1+k_1+\mu)^2(\delta+\sigma_4+\mu)}\left[\frac{k_2(k_1+\mu)}{k_2+\sigma_1+\mu}-\frac{(1-p)k_1\gamma_2}{\gamma_2+\sigma_3+\mu}\right]$$

so that, $\frac{\partial R_c}{\partial \gamma_1} < 0$ (> 0) iff $r_Q < r_{\gamma_1}$ $(r_Q > r_{\gamma_1})$ where

$$0 < r_{\gamma_1} = \frac{k_2+\sigma_1+\mu}{k_1+\mu}\left[\frac{r_A p k_1}{\sigma_2+\mu}+\frac{k_1(1-p)}{\gamma_2+\sigma_3+\mu}\right] + \frac{r_J(k_2+\sigma_1+\mu)}{(k_1+\mu)(\delta+\sigma_4+\mu)}\left[\frac{(1-p)k_1\gamma_2}{\gamma_2+\sigma_3+\mu}-\frac{k_2(k_1+\mu)}{k_2+\sigma_1+\mu}\right]$$

From the previous analysis, it is obvious that if the relative infectiousness of quarantine individuals r_Q will not cross the threshold value r_{γ_1}, then quarantining of exposed individuals results in reduction of the control reproduction number R_c and therefore reduction of the disease burden. On the other side, if $r_Q > r_{\gamma_1}$, then the control reproduction number R_c would rise due to the increase in the quarantine rate and thus the disease burden will also rise and therefore the use of quarantine in this scenario is harmful. The result is summarized in the following way:

Theorem 3.5. *For the model (2.8), the use of quarantine of the exposed individuals will have positive (negative) population-level impact if* $r_Q < r_{\gamma_1}$ $(r_Q > r_{\gamma_1})$.

Similarly, measuring the partial derivatives of R_c with respect to the isolation parameter $\gamma_2$is used to determine the effect of isolation of infected symptomatic individuals. Thus, we obtain

$$\frac{\partial R_c}{\partial \gamma_2} = \frac{r_J\beta(1-p)k_1}{(\gamma_1+k_1+\mu)(\gamma_2+\sigma_3+\mu)(\delta+\sigma_4+\mu)} - \frac{r_J\beta(1-p)k_1\gamma_2}{(\gamma_1+k_1+\mu)(\gamma_2+\sigma_3+\mu)^2(\delta+\sigma_4+\mu)}$$

$$- \frac{\beta k_1(1-p)}{(\gamma_1+k_1+\mu)(\gamma_2+\sigma_3+\mu)^2}$$

Thus, $\frac{\partial R_c}{\partial \gamma_2} < 0$ (> 0) iff $r_J < r_{\gamma_2}$ $(r_J > r_{\gamma_2})$ where

$$0 < r_{\gamma_2} = \frac{\delta+\sigma_4+\mu}{\sigma_3+\mu}$$

The use of isolation of infected symptomatic individuals will also be effective in controlling the disease in the population if the relative infectiousness of the isolated individuals r_J does not cross the threshold r_{γ_2}. The result is summarized below:

Theorem 3.6. *For the model (2.8), the use of isolation of infected symptomatic individuals will have positive (negative) population-level impact if* $r_J < r_{\gamma_2}$ $(r_J > r_{\gamma_2})$.

The control reproduction number R_c is a decreasing (non-decreasing) function of the quarantine and isolation parameters γ_1 and γ_2 if the conditions $r_Q < r_{\gamma_1}$ and $r_J < r_{\gamma_2}$ are respectively satisfied. See Fig. 7(a) and (b) obtained from model simulation in which the results correspond to the theoretical findings discussed.

3.6. Model without control and basic reproduction number

We consider the system in this section when there is no control mechanism, that is, in the absence of quarantined and isolated classes. Setting $\gamma_1 = \gamma_2 = 0$ in the model (2.8) give the following reduce model

$$\begin{aligned}
\frac{dS}{dt} &= \Pi - \frac{S(\beta I + r_A\beta A)}{\hat{N}} - \mu S,\\
\frac{dE}{dt} &= \frac{S(\beta I + r_A\beta A)}{\hat{N}} - (k_1+\mu)E,\\
\frac{dA}{dt} &= pk_1E - (\sigma_2+\mu)A,\\
\frac{dI}{dt} &= (1-p)k_1E - (\sigma_3+\mu)I,\\
\frac{dR}{dt} &= \sigma_2A + \sigma_3I - \mu R,
\end{aligned} \tag{3.7}$$

Where $\hat{N} = S+E+A+I+R$. The diseases-free equilibrium can be obtained for the system (3.7) by putting $E=0, A=0, I=0$, which is denoted by $P_2^0 = (S^0, 0, 0, 0, R^0)$, where

$$S^0 = \frac{\Pi}{\mu}, R^0 = 0.$$

We will follow the convention that the basic reproduction number is defined in the absence of control measure, denoted by R_0 whereas we calculate the control reproduction number when the control measure is in place. The basic reproduction number R_0 is defined as the expected number of secondary infections produced by a single infected individual in a fully susceptible population during his infectious period [8,25,30]. We calculate R_0 in the same way as we calculate R_c by using next generation operator method [54]. Now we calculate the jacobian of $\mathcal{F}$ and $\mathcal{V}$ at DFE P_2^0

$$F = \frac{\partial \mathcal{F}}{\partial X} = \begin{pmatrix} 0 & r_A\beta & \beta \\ 0 & 0 & 0 \\ 0 & 0 & 0 \end{pmatrix}, V = \frac{\partial \mathcal{V}}{\partial X} = \begin{pmatrix} \gamma_1+k_1+\mu & 0 & 0 \\ -pk_1 & \sigma_2+\mu & 0 \\ -(1-p)k_1 & 0 & \gamma_2+\sigma_3+\mu \end{pmatrix}.$$

Following [29], $R_0 = \rho(FV^{-1})$, where ρ is the spectral radius of the next-generation matrix (FV^{-1}). Thus, from the model (3.7), we have the following expression for R_0:

$$R_0 = \frac{r_A\beta pk_1}{(k_1+\mu)(\sigma_2+\mu)} + \frac{\beta k_1(1-p)}{(k_1+\mu)(\sigma_3+\mu)} \tag{3.8}$$

Thus, R_0 is R_c with $\gamma_1 = \gamma_2 = 0$. From, the expression of R_0 it is clear that it consists of two parts i.e, $\frac{r_A\beta pk_1}{(k_1+\mu)(\sigma_2+\mu)}$, $\frac{\beta k_1(1-p)}{(k_1+\mu)(\sigma_3+\mu)}$ which come from asymptomatic and symptomatic patients respectively. Also, note that when $p=0$ or all the COVID-19 patients are symptomatic the expression of R_0 only have the symptomatic part of the expression. On the other hand, when $p=1$ or all the patients are asymptomatic then the expression of R_0 only have the asymptomatic part of the expression. We list few expressions of R_0 from existing COVID-19 models in Table 2. The description of each parameters in the expressions can be found in the respective references. From these expressions, we can observe that the terms in the expression of R_0 are determined by the number of infectious compartments in the models. Suwardi et al. [9] has a single term as they have considered one infectious compartment whereas Sardar et al. [50], Monteiro et al. [42] and Monteiro [43] have two terms as they considered both asymptomatic and symptomatic patients. The expression of R_0 of our proposed model also has two terms representing contribution from asymptomatic and symptomatic patients. Similarly, Jayrold et al. [10] and Silvio et al. [48] have got three terms in the expression as they considered three infectious compartments in their models.

Table 2
Some previously reported expressions of R_0 for COVID-19.

Study	R_0	Epidemiological meaning
Suwardi et al. [9] (*SEIR*)	$\frac{\alpha\beta\mu}{(\mu+\beta)(\mu+\nu)(\mu_i+\delta+\mu)}$	The term $\frac{\alpha}{\mu+\beta}$ is the contact rate with exposed people. An infected individual spends on average a time $\frac{1}{\mu_i+\delta+\mu}$ in the infective compartment before entering in the recovered class. R_0 is proportional to $\frac{1}{\nu+\mu}$ which represent the proportion of susceptibles who can not get the disease.
Sardar et al. [50] (*SEAICR*)	$\frac{\beta_1\kappa\sigma}{(\mu+\sigma)(\gamma_2+\tau+\mu)} + \frac{\rho\beta_1(1-\kappa)\sigma}{(\mu+\sigma)(\gamma_1+\mu)}$	The two terms of the expression are due to asymptomatic and symptomatic patients respectively. An exposed individual spends on average a time $\frac{1}{\mu+\sigma}$ in the exposed class before entering in the asymptomatic and symptomatic class with rate $(1-\kappa)\sigma$ and $\kappa\sigma$ respectively. An asymptomatic and symptomatic individual spends on average a time $\frac{1}{\gamma_1+\mu}$ and $\frac{1}{\gamma_2+\tau+\mu}$ before entering in the hospitalized class.
Jayrold et al. [10] (*SEI$_a$I$_s$UR*)	$\omega(\frac{\beta_e}{\delta_e+\nu_e} + \frac{f\beta_s}{\gamma_s+\mu_s+\nu_s} + \frac{(1-f)\beta_a}{\gamma_a})\frac{S^*}{N^*}$	The term $\frac{\omega\beta_e}{\delta_e+\nu_e}$ represents the contact rate with exposed during the average latency period $\frac{1}{\delta_e+\nu_e}$. The term $\frac{\omega f\beta_s}{\gamma_s+\mu_s+\nu_s}$ is the contact rate with symptomatic during the average infection period, and the last one is the part of asymptomatic.
Silvio et al. [48] (*SEI$_A$I$_S$I$_D$RD*)	$\frac{\alpha\epsilon}{\zeta+\eta_A} + \frac{\beta(1-\epsilon)}{\theta_s+\eta_s+\kappa} + \frac{\gamma}{\theta_D+\kappa_D}[\frac{\epsilon}{\zeta+\eta_A}\eta_A + \frac{1-\epsilon}{\theta_s+\eta_s+\kappa}\eta_s]$	An asymptomatic and symptomatic individual spends on average a time $\frac{1}{\delta}$ in the exposed compartment before entering in the infective asymptomatic and symptomatic compartment with rate $\epsilon\delta$ and $(1-\epsilon)\delta$ respectively, where she/he spends on average a time $\frac{1}{\zeta+\eta_A}$ and $\frac{1}{\theta_s+\eta_s+\kappa}$, occurs with a rate β. Finally a diagnosed individual, that spends on average a time $\frac{1}{\theta_D+\kappa_D}$ and can infect with rate γ, can either be originated by an asymptomatic symptomatic individual with rate η_A and η_s respectively.
L.H.A. Monteiro et al. [43] (*SAIR*)	$\frac{xa_1N}{b_1+c_1} + \frac{(1-x)a_2N}{b_2+c_2}$	The two terms of the expression are due to asymptomatic and symptomatic patients respectively. The term $\frac{xa_1N}{b_1+c_1}$ represents the contact rate with asymptomatic during the average time period $\frac{1}{b_1+c_1}$. The term $\frac{(1-x)a_2N}{b_2+c_2}$ represents the contact rate with symptomatic during the average time period $\frac{1}{b_2+c_2}$.
L.H.A. Monteiro [42] (*SAIR*)	$\lvert\frac{nN}{2p} + \sqrt{(\frac{nN}{2p})^2 + \frac{mN^2}{p}}\rvert$	In this case, two terms of the expression consist of mixed effects from both symptomatic and asymptomatic patients.

3.6.1. Stability of DFE of the model3.7

Theorem 3.7. *The diseases free equilibrium (DFE) $P_2^0 = (S^0, 0, 0, 0, R^0)$ of the system (3.7) is locally asymptotically stable if $R_0 < 1$ and unstable if $R_0 > 1$.*

Proof. We calculate the Jacobian of the system (3.7) at DFE P_2^0, is given by

$$J_{P_2^0} = \begin{pmatrix} -\mu & 0 & -r_A\beta & -\beta & 0 \\ 0 & -(k_1+\mu) & r_A\beta & \beta & 0 \\ 0 & pk_1 & -(\sigma_2+\mu) & 0 & 0 \\ 0 & (1-p)k_1 & 0 & -(\sigma_3+\mu) & 0 \\ 0 & 0 & \sigma_2 & \sigma_3 & -\mu \end{pmatrix}$$

Let λ be the eigenvalue of the matrix $J_{P_2^0}$. Then the characteristic equation is given by $det(J_{P_2^0} - \lambda I) = 0$.

$$\Rightarrow r_A\beta pk_1(\lambda+\sigma_3+\mu) + \beta k_1[(1-p)(\lambda+\sigma_2+\mu)] - (\lambda+k_1+\mu)(\lambda+\sigma_2+\mu)(\lambda+\sigma_3+\mu) = 0.$$

which implies

$$\frac{r_A\beta pk_1}{(\lambda+k_1+\mu)(\lambda+\sigma_2+\mu)} + \frac{\beta k_1(1-p)}{(\lambda+k_1+\mu)(\lambda+\sigma_3+\mu)} = 1 = G_2(\lambda)(say).$$

We rewrite $G_2(\lambda)$ as $G_2(\lambda) = G_{21}(\lambda) + G_{22}(\lambda)$

Now if $Re(\lambda) \geq 0$, $\lambda = x + iy$, then

$$|G_{21}(\lambda)| \leq \frac{r_A\beta pk_1}{|\lambda+k_1+\mu||\lambda+\sigma_2+\mu|} \leq G_{21}(x) \leq G_{21}(0)$$

$$|G_{22}(\lambda)| \leq \frac{\beta k_1(1-p)}{|\lambda+k_1+\mu||\lambda+\sigma_3+\mu|} \leq G_{22}(x) \leq G_{22}(0)$$

Then $G_{21}(0) + G_{22}(0) = G_2(0) = R_0 < 1$, which implies $|G_2(\lambda)| \leq 1$.

Thus for $R_0 < 1$, all the eigenvalues of the characteristics equation $G_2(\lambda) = 1$ has negative real parts.

Therefore if $R_0 < 1$, all eigenvalues are negative and hence DFE P_2^0 is locally asymptotically stable.

Now if we consider $R_0 > 1$ i.e $G_2(0) > 1$, then

$$\lim_{\lambda\to\infty} G_2(\lambda) = 0.$$

Then there exist $\lambda^* > 0$ such that $G_2(\lambda^*) = 1$.

That means there exist positive eigenvalue $\lambda^* > 0$ of the Jacobian matrix.

Hence DFE P_2^0 is unstable whenever $R_0 > 1$. □

Theorem 3.8. *The diseases free equilibrium (DFE) $P_2^0 = (S^0, 0, 0, 0, R^0)$ is globally asymptotically stable for the system (3.7) if $R_0 < 1$ and unstable if $R_0 > 1$.*

Proof. We rewrite the system (3.7)as

$$\frac{dX}{dt} = F_1(X, V)$$
$$\frac{dV}{dt} = G_1(X, V), G_1(X, 0) = 0$$

where $X = (S, R) \in R_2$ (the number of uninfected individuals compartments), $V = (E, A, I) \in R_3$ (the number of infected individuals compartments), and $P_2^0 = (\frac{\Pi}{\mu}, 0, 0, 0, 0)$ is the DFE of the system (3.7). The global stability of the DFE is guaranteed if the following two conditions are satisfied:

1. For $\frac{dX}{dt} = F_1(X, 0)$, X^* is globally asymptotically stable,
2. $G_1(X, V) = BV - \widehat{G}_1(X, V)$, $\widehat{G}_1(X, V) \geq 0$ for $(X, V) \in \hat{\Omega}$,

where $B = D_V G_1(X^*, 0)$ is a Metzler matrix and $\hat{\Omega}$ is the positively invariant set with respect to the model (3.7). Following Castillo-Chavez et al [13], we check for aforementioned conditions.

For system (3.7),

$$F_1(X, 0) = \begin{matrix} \Pi - \mu S, \\ 0 \end{matrix}$$

$$B = \begin{matrix} -(k_1 + \mu) & r_A\beta & \beta \\ pk_1 & -(\sigma_2 + \mu) & 0 \\ (1-p)k_1 & 0 & -(\sigma_3 + \mu) \end{matrix}$$

and

$$\widehat{G}_1(X, V) = \begin{pmatrix} r_A\beta A(1 - \frac{S}{\hat{N}}) + \beta I(1 - \frac{S}{\hat{N}}) \\ 0 \\ 0 \end{pmatrix}.$$

Clearly, $\widehat{G}_1(X, V) \geq 0$ whenever the state variables are inside $\hat{\Omega}$. Also it is clear that $X^* = (\frac{\Pi}{\mu}, 0)$ is a globally asymptotically stable equilibrium of the system $\frac{dX}{dt} = F_1(X, 0)$. Hence, the theorem follows. □

3.6.2. Existence and local stability of endemic equilibrium

In this section, the existence of the endemic equilibrium of the model (3.7) is established. Let us denote

$$h_1 = k_1 + \mu, h_2 = \sigma_2 + \mu, h_3 = \sigma_3 + \mu.$$

Let $P_2^* = (\hat{S}, \hat{E}, \hat{A}, \hat{I}, \hat{R})$ represents any arbitrary endemic equilibrium point (EEP) of the model (3.7). Further, define

$$\lambda^* = \frac{\beta(\hat{I} + r_A\hat{A})}{\hat{N}} \tag{3.9}$$

It follows, by solving the equations in (3.7) at steady-state, that

$$\hat{S} = \frac{\Pi}{\lambda^* + \mu}, \hat{E} = \frac{\lambda^*\hat{S}}{h_1}, \hat{A} = \frac{pk_1\lambda^*\hat{S}}{h_1h_2}, \tag{3.10}$$
$$\hat{I} = \frac{(1-p)k_1\lambda^*\hat{S}}{h_1h_3}, \hat{R} = \frac{\lambda^*\hat{S}[pk_1\sigma_2h_3 + (1-p)k_1\sigma_3h_2]}{\mu h_1h_2h_3}$$

Substituting the expression in (3.10) into (3.9) shows that the non-zero equilibrium of the model (3.7) satisfy the following linear equation, in terms of λ^*:

$$X\lambda^* + Y = 0 \tag{3.11}$$

where

$$X = \mu h_2h_3 + \mu pk_1h_3 + \mu(1-p)k_1h_2 + \sigma_2pk_1h_3 + (1-p)k_1\sigma_3h_2$$
$$Y = \mu h_1h_2h_3(1 - R_0)$$

Since $X > 0$, $\mu > 0$, $h_1 > 0$, $h_2 > 0$ and $h_3 > 0$, it is clear that the model (3.7) has a unique endemic equilibrium point (EEP) whenever $R_0 > 1$ and no positive endemic equilibrium point whenever $R_0 < 1$. This rules out the possibility of the existence

Table 3
Estimated initial population sizes for the UK.

Initial values	Value	Source
$S(0)$	20,341,362	Estimated
$E(0)$	561	Estimated
$Q(0)$	2718	Assumed
$A(0)$	1092	Estimated
$I(0)$	3	Estimated
$J(0)$	751	Data
$R(0)$	10	Assumed

of equilibrium other than DFE whenever $R_0 < 1$. Furthermore, it can be shown that, the DFE P_2^0 of the model (3.7) is globally asymptotically stable (GAS) whenever $R_0 < 1$.

From the above discussion we have concluded that

Theorem 3.9. *The endemic equilibrium P_2^* is locally asymptotically stable if $R_0 > 1$.*

Proof. A straightforward procedure same as the proof of Theorem 3.4 will prove this theorem. □

4. Model Calibration and epidemic potentials

We calibrated our model (2.8) to the daily new COVID-19 cases for the UK. Daily COVID-19 cases are collected for the period 1 July, 2020 - 4 December, 2020 [4]. We divide the 157 data points into training periods and testing periods, viz., 1 July - 20 November and 21 November - 4 December respectively. We fit the model (2.8) to daily new isolated cases of COVID-19 in the UK. Due to the highly transmissible virus, the notified cases are immediately isolated, and therefore it is convenient to fit the isolated cases to reported data.

Also, we fit the model (2.8) to cumulative isolated cases of COVID-19. We estimate the diseases transmission rates by humans, β, quarantine rate of exposed individuals, γ_1, isolation rate of infected individual, γ_2, rate at which quarantined individuals are isolated, k_2, recovery rate from quarantined individuals, σ_1, recovery rate from asymptomatic individuals, σ_2, recovery rate from isolated individuals, σ_4, and initial population sizes. The COVID-19 data are fitted using the optimization function 'fminsearchbnd' (MATLAB, R2017a). The estimated parameters are given in Table 1. We also estimate the initial conditions of the human population and the estimated values are given by Table 3. The fitting of the daily isolated COVID-19 cases in the UK are displayed in Fig. 3.

Using these estimated parameters and the fixed parameters from Table 1, we calculate the basic reproduction numbers (R_0) and control reproduction numbers (R_c) for the UK. The values for R_0 and R_c are found to be 1.7291 and 1.5549 respectively. R_c value is above unity, which indicates that they should increase the control interventions to limit future COVID-19 cases.

5. Short-term predictions

In this section, the short-term prediction capability of the model 2.8 is studied. Using parameters form Tables 1 and 3, we simulate the newly isolated COVID-19 cases for the period 21 November, 2020 - 4 December, 2020 to check the accuracy of the predictions. Next, 10-day-ahead predictions are reported for the UK. The short-term prediction for the UK is depicted in Fig. 4.

We calculate two performance metrics, namely Mean Absolute Error (MAE) and Root Mean Square Error (RMSE) to assess the accuracy of the predictions. This is defined using a set of performance metrics as follows:

Mean Absolute Error (MAE):

$$MAE = \frac{1}{N_p}\sum_{i=1}^{N_p}|Y(i) - \hat{Y}(i)|$$

Root Mean Square Error (RMSE):

$$RMSE = \sqrt{\frac{1}{N_p}\sum_{i=1}^{N_p}(Y(i) - \hat{Y}(i))^2}$$

where $Y(i)$ represent original cases, $\hat{Y(i)}$ are predicted values and N_p represents the sample size of the data. These performance metrics are found to be MAE=3522 and RMSE=4227. We found that the model performs excellently in case of the UK. The decreasing trend of newly isolated COVID-19 cases is also well captured by the model.

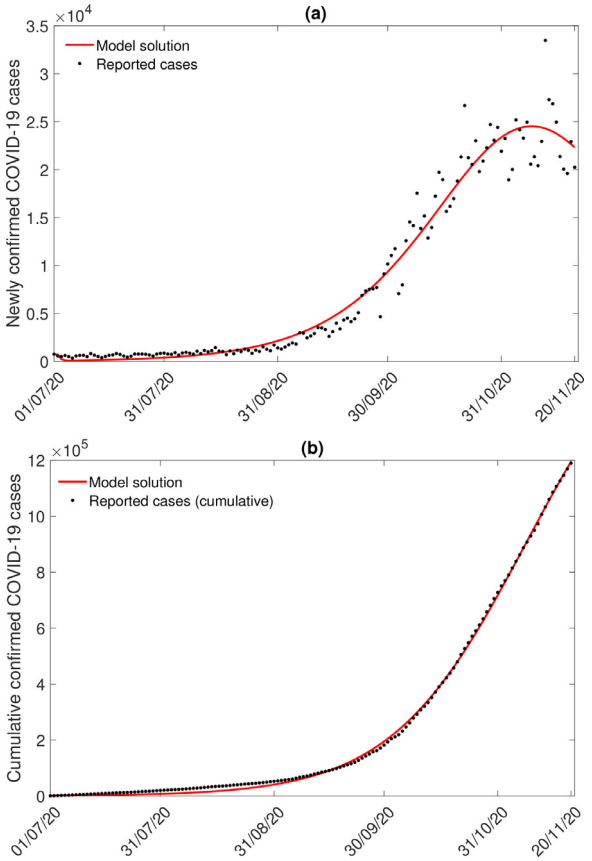

Fig. 3. (a) Model solutions fitted to daily new isolated COVID cases in the UK. (b) Model fitting with cumulative COVID-19 cases in the UK. Observed data points are shown in black circle and the solid red line depicts the model solutions. (For interpretation of the references to color in this figure legend, the reader is referred to the web version of this article.)

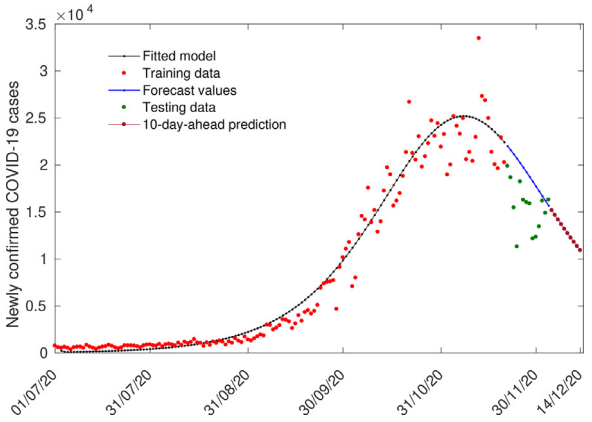

Fig. 4. Short term predictions for the UK. The blue line represent the predicted new isolated COVID cases while the solid dots are the actual cases. (For interpretation of the references to color in this figure legend, the reader is referred to the web version of this article.)

6. Control strategies

In order to get an overview of the most influential parameters, we compute the normalized sensitivity indices of the model parameters with respect to R_c. We have chosen parameters transmission rate between human population β, the control related parameters, γ_1, γ_2 and k_2, the recovery rates from quarantine individuals σ_1, asymptomatic individuals σ_2 and isolated individuals σ_4 and the effect of diseases induced mortality rate δ for sensitivity analysis. We compute normalized forward sensitivity indices of these parameters with respect to the control reproduction number R_c. We use

Table 4
Normalized sensitivity indices of some parameters of the model 2.8.

$X_{R_c}^{\beta}$	$X_{R_c}^{\gamma_1}$	$X_{R_c}^{\gamma_2}$	$X_{R_c}^{k_2}$	$X_{R_c}^{\sigma_1}$	$X_{R_c}^{\sigma_2}$	$X_{R_c}^{\sigma_4}$	$X_{R_c}^{\delta}$
1.0000	0.0964	0.0344	0.0033	0.0402	0.3214	0.1358	0.0005

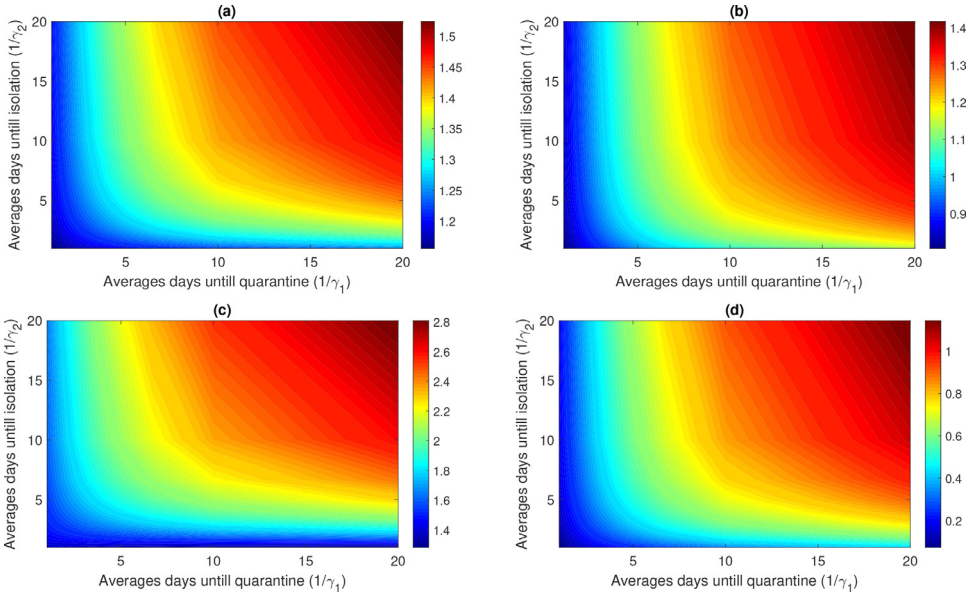

Fig. 5. Contour plots of R_c versus average days to quarantine $(1/\gamma_1)$ and isolation $(1/\gamma_2)$ for the UK, (a) in the presence of both modification factors for quarantined (r_Q) and isolation (r_J); (b) in the presence of modification factors for isolation (r_J) only; (c) in the presence of modification factors for quarantined (r_Q) only and (d) in the absence of both modification factors for quarantined (r_Q) and isolation (r_J). All parameter values other than γ_1 and γ_2 are given in Table 1.

the parameters from Tables 1 and 3. However, the mathematical definition of the normalized forward sensitivity index of a variable m with respect to a parameter τ (where m depends explicitly on the parameter τ) is given as:

$$X_m^{\tau} = \frac{\partial m}{\partial \tau} \times \frac{\tau}{m}.$$

The sensitivity indices of R_c with respect to the parameters β, γ_1, γ_2, k_2, σ_1, σ_2, σ_4 and δ are given by Table 4.

The fact that $X_{R_c}^{\beta} = 1$ means that if we increase 1% in β, keeping other parameters be fixed, will produce 1% increase in R_c. Similarly, $X_{R_c}^{\sigma_2} = -0.3214$ means increasing the parameter σ_2 by 1%, the value of R_c will be decreased by 0.3214% keeping the value of other parameters fixed. Therefore, the transmission rate between susceptible humans and COVID-19 infected humans is positively correlated and the recovery rate from asymptomatic class is negatively correlated with respect to control reproduction number respectively.

In addition, we draw the contour plots of R_c with respect to the parameters γ_1 and γ_2 for the model (2.8) to investigate the effect of the control parameters on control reproduction number R_c, see Fig. 5.

The contour plots of Fig. 5 show the dependence of R_c on the quarantine rate γ_1 and the isolation rate γ_2 for the UK. The axes of these plots are given as average days from exposed to quarantine $(1/\gamma_1)$ and average days from starting of symptoms to isolation $(1/\gamma_2)$. For both cases, the contours show that increasing γ_1 and γ_2 reduces the amount of control reproduction number R_c and, therefore, COVID cases. We find that quarantine and isolation are not sufficient to control the outbreak (see Fig. 5(a) and (c)). With these parameter values, as γ_1 increases, R_c decreases and similarly, when γ_2 increases, R_c decreases. But, in both cases $R_c > 1$, and therefore the disease will persist in the population (i.e. the above control measures cannot lead to effective control of the epidemic). By contrast, our study shows that when the modification factor for quarantine become zero (so that $r_Q = 0$), the outbreak can be controlled (see Fig. 5(b) and (d)). From the above finding, it follows that neither the quarantine of exposed individuals nor the isolation of symptomatic individuals will prevent the disease with the high value of the modification factor for quarantine. This control can be obtained by a significant reduction in COVID transmission during quarantine (that is reducing rQ).

Furthermore, we study the effect of the parameters modification factor for quarantined individuals (r_Q), modification factor for isolated individuals (r_J) and transmission rate (β) on the cumulative new isolated COVID-19 cases (J_{cum}) in the UK. The cumulative number of isolated cases has been computed at day 100 (chosen arbitrarily). The effect of controllable parameters on (J_{cum}) are shown in Fig. 6.

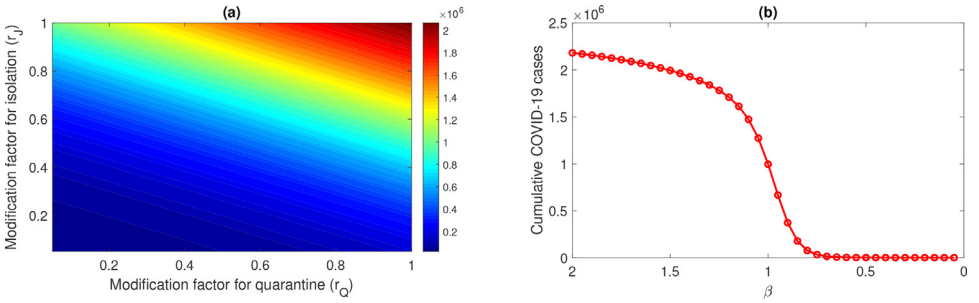

Fig. 6. Effect of controllable parameters γ_1, γ_2 and β on the cumulative number of isolated COVID-19 cases. The left panel shows the variability of the J_{cum} with respect to $\frac{1}{\gamma_1}$ and $\frac{1}{\gamma_2}$. The right panel shows J_{cum} with decreasing transmission rate β.

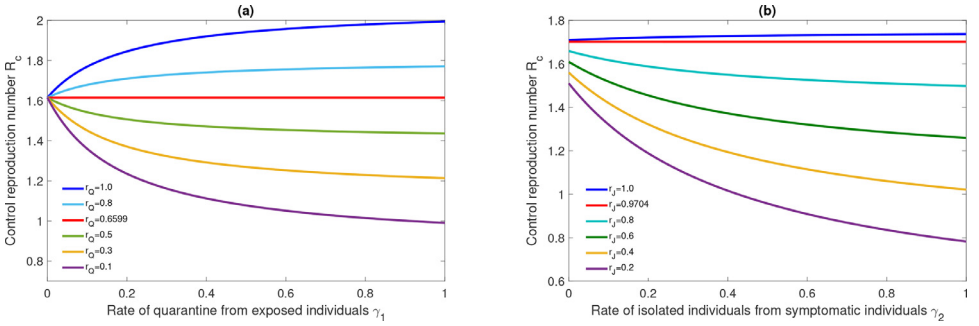

Fig. 7. Effect of isolation parameters γ_1 and γ_2 on control reproduction number R_c.

We observe that all the three parameters have a significant effect on the cumulative outcome of the epidemic. From Fig. 6(a) it is clear that decrease in the modification factor for quarantined and isolated individuals will significantly reduce the value of J_{cum}. On the other hand, Fig. 6(b) indicates, reduction in transmission rate will also slow down the epidemic significantly. These results point out that all the three control measures are quite effective in the reduction of the COVID-19 cases in the UK. Thus, quarantine and isolation efficacy should be increased by means of proper hygiene and personal protection by health care stuffs. Additionally, the transmission coefficient can be reduced by avoiding contacts with suspected COVID-19 infected cases.

Furthermore, We numerically calculated the thresholds r_{γ_1} and r_{γ_2} for the UK. The analytical expression of the thresholds are given in subsection (3.5). The effectiveness of quarantine and isolation depends on the values of the modification parameters r_Q and r_J for the reduction of infected individuals. The threshold value of r_Q corresponding to quarantine parameter γ_1 is $r_{\gamma_1} = 0.6599$ and the threshold value of r_J corresponding to isolation parameter γ_2 is $r_{\gamma_2} = 0.9704$.

From Fig. 7(a) it is clear that quarantine parameter γ_1 has positive population-level impact (R_c decreases with increase in γ_1) for $r_Q < 0.6599$ and have negative population level impact for $r_Q > 0.6599$. Similarly from the Fig. 7(b), it is clear that, isolation has positive level impact for $r_J < 0.9704$, whereas isolation has negative impact if $r_J > 0.9704$. This result indicate that isolation and quarantine programs should run effective so that the modification parameters remain below the above mentioned threshold.

7. Conclusions

During the period of an epidemic when human-to-human transmission is established and reported cases of COVID-19 are rising worldwide, forecasting is of utmost importance for health care planning and control of the virus with limited resources. In this study, we have formulated and analyzed a compartmental epidemic model of COVID-19 to predict and control the outbreak. The basic reproduction number and control reproduction number are calculated for the proposed model. It is also shown that whenever $R_0 < 1$, the DFE of the model without control is globally asymptotically stable. The efficacy of quarantine of exposed individuals and isolation of infected symptomatic individuals depends on the size of the modification parameter to reduce the infectiousness of exposed (r_Q) and isolated (r_J) individuals. The usage of quarantine and isolation will have positive population-level impact if $r_Q < r_{\gamma_1}$ and $r_J < r_{\gamma_2}$ respectively. We calibrated the proposed model to fit daily data from the UK. Using the parameter estimates, we then found the basic and control reproduction numbers for the UK. Our findings suggest that independent self-sustaining human-to-human spread ($R_0 > 1$, $R_c > 1$) is already present in the UK. The estimates of the control reproduction number indicate that sustained control interventions are necessary to reduce the future COVID-19 cases. The health care agencies should focus on the successful implementation of control mechanisms to reduce the burden of the disease.

The calibrated model then have checked for short-term predictability. It is seen that the model performs excellently (Fig. 4). The model predicted that the new cases in the UK will show a decreasing trend in the near future. However, if the control measures are increased (or R_c is decreased below unity to ensure GAS of the DFE) and maintained efficiently, the subsequent outbreaks can be controlled.

Having an estimate of the parameters and prediction results, we performed control intervention related numerical experiments. Sensitivity analysis reveals that the transmission rate is positively correlated and quarantine and isolation rates are negatively correlated with respect to control reproduction number. This indicates that increasing quarantine and isolation rates and decreasing transmission rate will decrease the control reproduction number and consequently will reduce the disease burden.

While investigating the contour plots 5, we found that effective management of quarantined individuals is more effective than management of isolated individuals to reduce the control reproduction number below unity. Thus if limited resources are available, then investing in the quarantined individuals will be more fruitful in terms of reduction of cases.

Finally, we studied the effect of modification factor for quarantined population, modification factor for isolated population and transmission rate on the newly infected symptomatic COVID-19 cases. Numerical results show that all the three control measures are quite effective in reduction of the COVID-19 cases in the UK (Fig. 6). The threshold analysis reinforce that the quarantine and isolation efficacy should be increased to reduce the epidemic (Fig. 7). Thus, quarantine and isolation efficacy should be increased using proper hygiene and personal protection by health care stuffs. Additionally, the transmission coefficient can be reduced by avoiding contacts with suspected COVID-19 infected cases.

In summary, our study suggests that COVID-19 has a potential to be endemic for quite a long period but it is controllable by social distancing measures and efficiency in quarantine and isolation. Moreover, if limited resources are available, then investing in the quarantined individuals will be more fruitful in terms of the reduction of cases. The ongoing control interventions should be adequately funded and monitored by the health ministry. Health care officials should supply medications, protective masks and necessary human resources in the affected areas.

Acknowledgements

Sk Shahid Nadim receives senior research fellowship from CSIR, Government of India, New Delhi. Research of Indrajit Ghosh is supported by National Board for Higher Mathematics (NBHM) postdoctoral fellowship (Ref. No. 0204/3/2020/R & D-II/2458). The authors thank the learned reviewers for the insightful comments that have improved the paper.

References

[1] WHO. Coronavirus disease (covid-19) outbreak, 2019, (https://www.who.int/emergencies/diseases/novel-coronavirus-2019). Retrieved : 2020-03-04.
[2] Wuhan wet market closes amid pneumonia outbreak, 2019, (https://www.chinadaily.com.cn/a/202001/01/WS5e0c6a49a310cf3e35581e30.html). Retrieved : 2020-03-04.
[3] Centers for disease control and prevention: 2019 novel coronavirus, 2020, (https://www.cdc.gov/coronavirus/2019-ncov). Retrieved : 2020-03-10.
[4] COVID-19 coronavirus outbreak, 2020, (https://www.worldometers.info/coronavirus/repro). Retrieved : 2020-03-04.
[5] Life expectancy at birth, total (years) - china, 2020, (https://data.worldbank.org/indicator/SP.DYN.LE00.IN?locations=CN). Retrieved : 2020-02-15.
[6] Nowcasting and Forecasting the Wuhan 2019-nCoV Outbreak. available online:, 2020, (https://files.sph.hku.hk/download/wuhan_exportation_preprint.pdf). Retrieved : 2020-03-04.
[7] D. Aldila, S.H.A. Khoshnaw, E. Safitri, Y.R. Anwar, A.R.Q. Bakry, B.M. Samiadji, D.A. Anugerah, M.F.A. Gh, I.D. Ayulani, S.N. Salim, A mathematical study on the spread of COVID-19 considering social distancing and rapid assessment: the case of jakarta, indonesia, Chaos Solitons Fract. 139 (2020) 110042.
[8] R.M. Anderson, M. Robert, May. infectious diseases of humans: dynamics and control, Oxf. Sci. Publ. 36 (1991) 118.
[9] S. Annas, M.I. Pratama, M. Rifandi, W. Sanusi, S. Side, Stability analysis and numerical simulation of SEIR model for pandemic COVID-19 spread in indonesia, Chaos Solitons Fract. 139 (2020) 110072.
[10] J.P. Arcede, R.L. Caga-Anan, C.Q. Mentuda, Y. Mammeri, Accounting for symptomatic and asymptomatic in a SEIR-type model of COVID-19, Math. Model. Nat. Phenom. 15 (2020) 34.
[11] I.I. Bogoch, A. Watts, A. Thomas-Bachli, C. Huber, M.U.G. Kraemer, K. Khan, Pneumonia of unknown aetiology in Wuhan, China: potential for international spread via commercial air travel, J. Travel Med. 27 (2) (2020) taaa008.
[12] T. Britton, F. Ball, P. Trapman, A mathematical model reveals the influence of population heterogeneity on herd immunity to SARS-cov-2, Science 369 (6505) (2020) 846–849.
[13] C. Castillo-Chavez, Z. Feng, W. Huang, On the computation of ro and its role on, mathematical approaches for emerging and reemerging infectious diseases: an introduction 1(2002) 229.
[14] C. Castillo-Chavez, B. Song, Dynamical models of tuberculosis and their applications, Math. Biosci. Eng. 1 (2) (2004) 361.
[15] T. Chakraborty, I. Ghosh, Real-time forecasts and risk assessment of novel coronavirus (COVID-19) cases: a data-driven analysis, Chaos Solitons Fract. 135 (2020) 109850.
[16] J.F.-W. Chan, S. Yuan, K.-H. Kok, K.K.-W. To, H. Chu, J. Yang, F. Xing, J. Liu, C.C.-Y. Yip, R.W.-S. Poon, et al., A familial cluster of pneumonia associated with the 2019 novel coronavirus indicating person-to-person transmission: a study of a family cluster, Lancet 395 (10223) (2020) 514–523.
[17] T.-M. Chen, J. Rui, Q.-P. Wang, Z.-Y. Zhao, J.-A. Cui, L. Yin, A mathematical model for simulating the phase-based transmissibility of a novel coronavirus, Infect. Dis. Poverty 9 (1) (2020) 1–8.
[18] G. Chowell, S.M. Bertozzi, M.A. Colchero, H. Lopez-Gatell, C. Alpuche-Aranda, M. Hernandez, M.A. Miller, Severe respiratory disease concurrent with the circulation of h1n1 influenza, N. Engl. J. Med. 361 (7) (2009) 674–679.
[19] G. Chowell, S. Echevarría-Zuno, C. Viboud, L. Simonsen, J. Tamerius, M.A. Miller, V.H. Borja-Aburto, Characterizing the epidemiology of the 2009 influenza a/h1n1 pandemic in mexico, PLoS Med. 8 (5) (2011).
[20] A. Clark, M. Jit, C. Warren-Gash, B. Guthrie, H.H.X. Wang, S.W. Mercer, C. Sanderson, M. McKee, C. Troeger, K.L. Ong, et al., Global, regional, and national estimates of the population at increased risk of severe COVID-19 due to underlying health conditions in 2020: a modelling study, Lancet Glob. Health 8 (8) (2020) e1003–e1017.
[21] B.J. Cowling, M. Park, V.J. Fang, P. Wu, G.M. Leung, J.T. Wu, Preliminary epidemiologic assessment of MERS-cov outbreak in south korea, may–june 2015, Euro surveillance: bulletin Europeen sur les maladies transmissibles, Eur. Commun. Dis. Bull. 20 (25) (2015).

[22] N.G. Davies, A.J. Kucharski, R.M. Eggo, A. Gimma, W.J. Edmunds, T. Jombart, K. O'Reilly, A. Endo, J. Hellewell, E.S. Nightingale, et al., Effects of non-pharmaceutical interventions on COVID-19 cases, deaths, and demand for hospital services in the UK: a modelling study, Lancet Public Health 5 (7) (2020) e375–e385.
[23] R.J. de Groot, S.C. Baker, R.S. Baric, C.S. Brown, C. Drosten, L. Enjuanes, R.A.M. Fouchier, M. Galiano, A.E. Gorbalenya, Z.A. Memish, et al., Commentary: middle east respiratory syndrome coronavirus (MERS-cov): announcement of the coronavirus study group, J. Virol. 87 (14) (2013) 7790–7792.
[24] M. De la Sen, R.P. Agarwal, A. Ibeas, S. Alonso-Quesada, On a generalized time-varying SEIR epidemic model with mixed point and distributed time–varying delays and combined regular and impulsive vaccination controls, Adv. Differ. Equ. 2010 (1) (2010) 281612.
[25] O. Diekmann, J.A.P. Heesterbeek, Mathematical Epidemiology of Infectious Diseases: Model Building, Analysis and Interpretation, 5, John Wiley & Sons, 2000.
[26] C. Fraser, C.A. Donnelly, S. Cauchemez, W.P. Hanage, M.D. Van Kerkhove, T.D. Hollingsworth, J. Griffin, R.F. Baggaley, H.E. Jenkins, E.J. Lyons, et al., Pandemic potential of a strain of influenza a (h1n1): early findings, Science 324 (5934) (2009) 1557–1561.
[27] L.E. Gralinski, V.D. Menachery, Return of the coronavirus: 2019-ncov, Viruses 12 (2) (2020) 135.
[28] A.B. Gumel, S. Ruan, T. Day, J. Watmough, F. Brauer, P. Van den Driessche, D. Gabrielson, C. Bowman, M.E. Alexander, S. Ardal, et al., Modelling strategies for controlling SARS outbreaks, Proc. R. Soc. Lond. Ser.B 271 (1554) (2004) 2223–2232.
[29] J.M. Heffernan, R.J. Smith, L.M. Wahl, Perspectives on the basic reproductive ratio, J. R. Soc. Interface 2 (4) (2005) 281–293.
[30] H.W. Hethcote, The mathematics of infectious diseases, SIAM Rev. 42 (4) (2000) 599–653.
[31] C. Huang, Y. Wang, X. Li, L. Ren, J. Zhao, Y. Hu, L. Zhang, G. Fan, J. Xu, X. Gu, et al., Clinical features of patients infected with 2019 novel coronavirus in Wuhan, China, Lancet 395 (10223) (2020) 497–506.
[32] N. Imai, I. Dorigatti, A. Cori, S. Riley, N.M. Ferguson, Estimating the potential total number of novel coronavirus cases in Wuhan city, China, 2020, 10.25561/77149.
[33] M. Jit, T. Jombart, E.S. Nightingale, A. Endo, S. Abbott, W.J. Edmunds, et al., Estimating number of cases and spread of coronavirus disease (COVID-19) using critical care admissions, United Kingdom, February to March 2020, Eurosurveillance 25 (18) (2020) 2000632.
[34] K.H. Kim, T.E. Tandi, J.W. Choi, J.M. Moon, M.S. Kim, Middle east respiratory syndrome coronavirus (MERS-cov) outbreak in South Korea, 2015: epidemiology, characteristics and public health implications, J. Hosp. Infect. 95 (2) (2017) 207–213.
[35] A.J. Kucharski, P. Klepac, A.J.K. Conlan, S.M. Kissler, M.L. Tang, H. Fry, J.R. Gog, W.J. Edmunds, J.C. Emery, G. Medley, et al., Effectiveness of isolation, testing, contact tracing, and physical distancing on reducing transmission of SARS-cov-2 in different settings: a mathematical modelling study, Lancet Infect. Dis. 20 (10) (2020) 1151–1160.
[36] A.J. Kucharski, T.W. Russell, C. Diamond, Y. Liu, J. Edmunds, S. Funk, R.M. Eggo, F. Sun, M. Jit, J.D. Munday, et al., Early dynamics of transmission and control of COVID-19: a mathematical modelling study, Lancet Infect. Dis. 20 (5) (2020) 553–558.
[37] K.O. Kwok, A. Tang, V.W.I. Wei, W.H. Park, E.K. Yeoh, S. Riley, Epidemic models of contact tracing: systematic review of transmission studies of severe acute respiratory syndrome and middle east respiratory syndrome, Comput. Struct. Biotechnol. J. 17 (2019) 186–194.
[38] S. Lai, I. Bogoch, N. Ruktanonchai, A. Watts, Y. Li, J. Yu, X. Lv, W. Yang, H. Yu, K. Khan, et al., Assessing spread risk of Wuhan novel coronavirus within and beyond China, January-April 2020: a travel network-based modelling study, medRxiv (2020).
[39] W. Li, M.J. Moore, N. Vasilieva, J. Sui, S.K. Wong, M.A. Berne, M. Somasundaran, J.L. Sullivan, K. Luzuriaga, T.C. Greenough, et al., Angiotensin-converting enzyme 2 is a functional receptor for the SARS coronavirus, Nature 426 (6965) (2003) 450–454.
[40] M. Lipsitch, T. Cohen, B. Cooper, J.M. Robins, S. Ma, L. James, G. Gopalakrishna, S.K. Chew, C.C. Tan, M.H. Samore, et al., Transmission dynamics and control of severe acute respiratory syndrome, Science 300 (5627) (2003) 1966–1970.
[41] R.M. May, Infectious Diseases of Humans: Dynamics and Control, Oxford University Press, 1991.
[42] L. Monteiro, An epidemiological model for SARS-cov-2, Ecol. Complex. 43 (2020) 100836.
[43] L. Monteiro, V.C. Fanti, A.S. Tessaro, On the spread of SARS-cov-2 under quarantine: astudy based on probabilistic cellular automaton, Ecol. Complex. 44 (2020) 100879.
[44] K. Muniz-Rodriguez, G. Chowell, C.-H. Cheung, D. Jia, P.-Y. Lai, Y. Lee, M. Liu, S.K. Ofori, K.M. Roosa, L. Simonsen, et al., Doubling time of the COVID-19 epidemic by Province, China, Emerging Infect. Dis. 26 (8) (2020) 1912.
[45] S.S. Nadim, J. Chattopadhyay, Occurrence of backward bifurcation and prediction of disease transmission with imperfect lockdown: a case study on COVID-19, Chaos Solitons Fract. 140 (2020) 110163.
[46] K. Rajagopal, N. Hasanzadeh, F. Parastesh, I.I. Hamarash, S. Jafari, I. Hussain, A fractional-order model for the novel coronavirus (COVID-19) outbreak, Nonlinear Dyn. 101 (1) (2020) 711–718.
[47] J.M. Read, J.R.E. Bridgen, D.A.T. Cummings, A. Ho, C.P. Jewell, Novel coronavirus 2019-ncov: early estimation of epidemiological parameters and epidemic predictions, MedRxiv (2020).
[48] S. Romano, A. Fierro, A. Liccardo, Beyond the peak: a deterministic compartment model for exploring the covid-19 evolution in italy, PLoS One 15 (11) (2020) e0241951.
[49] T. Sardar, I. Ghosh, X. Rodó, J. Chattopadhyay, A realistic two-strain model for MERS-cov infection uncovers the high risk for epidemic propagation, PLoS Negl. Trop. Dis. 14 (2) (2020) e0008065.
[50] T. Sardar, S.S. Nadim, S. Rana, J. Chattopadhyay, Assessment of lockdown effect in some states and overall india: a predictive mathematical study on COVID-19 outbreak, Chaos Solitons Fract. 139 (2020) 110078.
[51] B. Tang, N.L. Bragazzi, Q. Li, S. Tang, Y. Xiao, J. Wu, An updated estimation of the risk of transmission of the novel coronavirus (2019-ncov), Infect. Dis. Model. 5 (2020) 248–255.
[52] B. Tang, X. Wang, Q. Li, N.L. Bragazzi, S. Tang, Y. Xiao, J. Wu, Estimation of the transmission risk of the 2019-ncov and its implication for public health interventions, J. Clin. Med. 9 (2) (2020) 462.
[53] P. Van den Driessche, J. Watmough, Further notes on the basic reproduction number, in: Mathematical Epidemiology, Springer, 2008, pp. 159–178.
[54] P. Van den Driessche, J. Watmough, Reproduction numbers and sub-threshold endemic equilibria for compartmental models of disease transmission, Math. Biosci. 180 (1–2) (2002) 29–48.
[55] J.T. Wu, K. Leung, G.M. Leung, Nowcasting and forecasting the potential domestic and international spread of the 2019-ncov outbreak originating in Wuhan, China: a modelling study, Lancet 395 (10225) (2020) 689–697.
[56] X. Yang, L. Chen, J. Chen, Permanence and positive periodic solution for the single-species nonautonomous delay diffusive models, Comput. Math. Appl. 32 (4) (1996) 109–116.